### Title

A mussel-derived one component adhesive coacervate




### Journal

Acta Biomaterialia, 10(4)

### ISSN

1742-7061



### Authors

Wei, Wei
Tan, Yerpeng
Rodriguez, Nadine R Martinez
et al.



### Publication Date

2014-04-01

### DOI

10.1016/j.actbio.2013.09.007

Acta Biomaterialia 10 (2014) 1663–1670

Contents lists available at ScienceDirect

Acta Biomaterialia

journal homepage: www.elsevier.com/locate/actabiomat

# A mussel-derived one component adhesive coacervate ☆

Wei Wei [a], Yerpeng Tan [b], Nadine R. Martinez Rodriguez [c], Jing Yu [d], Jacob N. Israelachvili [a,d,*], J. Herbert Waite [a,b,c,*]

[a] Materials Research Laboratory, University of California, Santa Barbara, CA 93106, USA
[b] Biomolecular Science and Engineering Graduate Program, University of California, Santa Barbara, CA 93106, USA
[c] Department of Molecular, Cell and Development Biology, University of California, Santa Barbara, CA 93106, USA
[d] Department of Chemical Engineering, University of California, Santa Barbara, CA 93106, USA

ARTICLE INFO

*Article history:*
Available online 21 September 2013

*Keywords:*
Coacervate
Biological wet adhesion
Mussel foot protein
Interfacial energy
Hydrophobicity
Hydroxyapatite

ABSTRACT

Marine organisms process and deliver many of their underwater coatings and adhesives as complex fluids. In marine mussels one such fluid, secreted during the formation of adhesive plaques, consists of a concentrated colloidal suspension of a mussel foot protein (mfp) known as Mfp-3S. The results of this study suggest that Mfp-3S becomes a complex fluid by a liquid–liquid phase separation from equilibrium solution at a pH and ionic strength reminiscent of the conditions created by the mussel foot during plaque formation. The pH dependence of phase separation and its sensitivity indicate that inter-/intramolecular electrostatic interactions are partially responsible for driving the phase separation. Hydrophobic interactions between the non- polar Mfp-3S proteins provide another important driving force for coacervation. As complex coacervation typically results from charge–charge interactions between polyanions and polycations, Mfp-3S is thus unique in being the only known protein that coacervates with itself. The Mfp-3S coacervate was shown to have an effective interfacial energy of $\leqslant 1$ mJ m$^{-2}$, which explains its tendency to spread over or engulf most surfaces. Of particular interest to biomedical applications is the extremely high adsorption capacity of coacervated Mfp-3S on hydroxyapatite.



## 1. Introduction

One of the most fascinating aspects of the underwater adhesion of marine organisms such as mussels and sandcastle worms is the reliance on metastable, water-insoluble fluids that resist being dispersed in the surrounding seawater. In mussels these adhesive fluids consist of highly concentrated, intrinsically unstructured polyelectrolytes known as mussel foot proteins (mfps) that rapidly solidify upon equilibration with seawater. In sandcastle worm cement, given the presence of both polyanions (polyphosphoserine-rich protein) and polycations (lysine-rich proteins), fluid–fluid phase separation is modelled as complex coacervation leading to a polyelectrolyte-depleted equilibrium phase and a denser, protein-rich coacervate phase [1,2]. Complex coacervation results from the coulombic attraction and neutralization of oppositely charged polyelectrolytes coupled with the concomitant release of counterions [3] and confers unusual properties on the coacervate phase, including relatively high diffusion coefficients of the solute and solvent molecules, high concentrations, relatively low viscosity, and a low interfacial energy, all highly conducive to dispensing adhesives underwater [4–8]. Coacervates are used industrially in micro-encapsulation technology [9,10], and are particularly important in food processing, as well as drug and gene delivery [11–15]. Hydrogel formation can also be mediated by coacervation [16].

Polyanions are not known to be involved in mussel adhesion, thus the basis for fluid–fluid phase separation by mfps remains unknown. In this report we show that Mfp-3S (Fig. 1), a zwitterionic protein functioning as both adhesive primer and sealant in mussel adhesion [17], undergoes fluid–fluid phase separation under conditions identical to those imposed by the mussel foot during plaque formation. The outstanding interfacial adhesive and cohesive properties of Mfp-3S over a relatively wide pH range have been previously demonstrated using a surface forces apparatus (SFA) [17], and attributed to its abundant 3,4-dihydroxyphenylalanine (dopa) content and unique hydrophobic sequence. The strategy of achieving efficient phase separation and surface spreading by coacervation is very appealing in its simplicity, in part because it is only rarely observed in single protein solutions: only tropoelastin is known to undergo simple hydrophobically driven coacervation [18,19]. Mfp-3S provides an interesting counterpoint for

☆ Part of the Special Issue on Biological Materials, edited by Professors Thomas H. Barker and Sarah C. Heilshorn.

* Corresponding authors. Address: Department of Chemical Engineering, University of California, Santa Barbara, CA 93106, USA (J.N. Israelachvili). Address: Biomolecular Science and Engineering Graduate Program, University of California, Santa Barbara, CA 93106, USA (J.H. Waite).

*E-mail addresses:* jacob@engineering.ucsb.edu (J.N. Israelachvili), herbert.waite@lifesci.ucsb.edu (J.H. Waite).

1742-7061/$ - see front matter © 2013 Acta Materialia Inc. Published by Elsevier Ltd. All rights reserved.
http://dx.doi.org/10.1016/j.actbio.2013.09.007

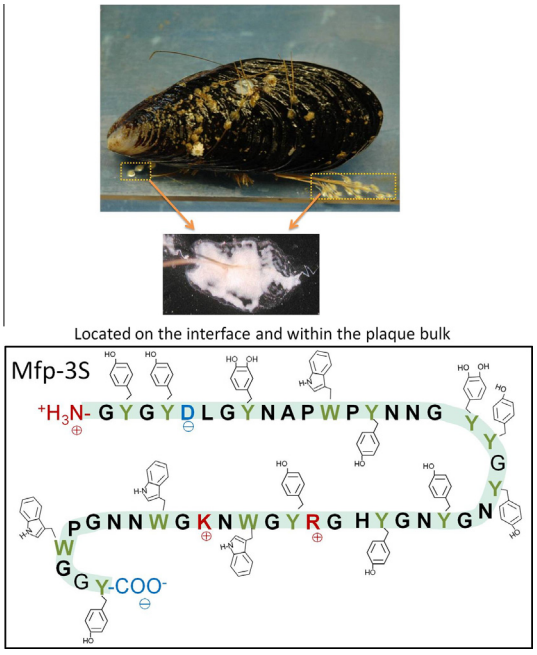


**Fig. 1.** A representative sequence of Mfp-3S from mussel plaque. Red, blue and green indicate positively charged, negatively charged and aromatic residues, respectively.

understanding the molecular requirements for single component coacervation. Based on how pH, ionic strength, and temperature affect Mfp-3S coacervation, we propose that the electrostatic and hydrophobic driving forces are uniquely balanced in the observed fluid–fluid phase separation of Mfp-3S. These forces will, of course, be subjected to much greater scrutiny as synthetic and recombinant mimics become more readily available. The relevance of coacervates to orthopaedic and dental materials was explored by investigating the adsorption of Mfp-3S coacervates on hydroxyapatite (HAP) ($Ca_{10}(PO_4)_6(OH)_2$,) surfaces.

## 2. Experimental section

### 2.1. Mfp-3S purification

Mfp-3S was purified from the plaques of California mussels, *Mytilus californianus*, as described elsewhere [20]. About 1000 accumulated plaques were thawed and homogenized in a small volume (5 ml per 200 plaques) of 5 vol.% acetic acid containing 8 M urea on ice using a small hand-held tissue grinder (Kontes, Vineland, NJ). The homogenate was centrifuged for 30 min at 20,000*g* and 4 °C. The soluble acetic acid/urea plaque extracts were subjected to reverse phase HPLC using a 260 × 7 mm RP-300 Aquapore column (Applied Biosciences Inc., Foster City, CA), eluted with a linear gradient of aqueous acetonitrile. The eluant was monitored continuously at 230 and 280 nm, and 1 ml fractions containing Mfp-3S were pooled and freeze-dried, injected into a Shodex-803 column (5 μm, 8 × 300 mm), which was equilibrated and eluted with 5% acetic acid in 0.1% trifluoroacetic acid. The eluant was monitored at 280 nm. Sample purity was assessed by acid urea PAGE, amino acid analysis, and MALDI time-of-flight mass spectrometry. Fractions with pure Mfp-3S were freeze-dried and redissolved in buffers for further studies. About 3 mg of Mfp-3S can be purified from 1000 freshly (within 24 h) secreted plaques.

### 2.2. Zeta potential

The zeta potentials of Mfp-3S in solution (~0.1 mg $ml^{-1}$) were obtained using a Malvern Nano ZS which is calibrated regularly using a Malvern Zeta Potential Transfer standard (P/N DTS1230, batch no. 380901). The zeta potentials of Mfp-3S were +23, +6, and −0.8 mV, respectively, in pH 5.5, 6.5 and 7.5 buffer at 100 mM ionic strength.

### 2.3. Mfp-3S self-coacervation and turbidity measurement

Stock solutions of 1 mg $ml^{-1}$ Mfp-3S were prepared in 10 mM acetic acid buffer (pH 3). The final protein concentration was fixed at 0.1 mg $ml^{-1}$ by adding stock solution to buffer at a volume ratio of 1:9 (stock:buffer). Coacervation of Mfp-3S at different buffer conditions was measured turbidimetrically at 600 nm by UV-vis spectrophotometry. Mfp-3S absorbance was negligible at 600 nm. The relative turbidity is defined as $\ln(T/T_0)$, where $T$ and $T_0$ are the light transmittance with and without sample, respectively [21].

### 2.4. Microscopy

The turbidity associated with coacervate droplet formation was visually inspected by inverted light microscopy. The protein distribution was also investigated using an Olympus model IX81 DSU fluorescence microscope (Olympus, Tokyo, Japan). Images were taken with an ImagEM camera (C9100-13, Hamamatsu, Shizuoka, Japan) under the control of MetaMorph software (Olympus). The desired excitation and emission wavelengths were obtained using a mercury bulb combined with a 89000 Sedat Quad Filter Set (Chroma Tech. Corp.).

### 2.5. Quantification of adsorbed coacervate by amino acid analysis

A scaled-up version of a microscopic slide with coverslip was made using two rectangular glass slides as follows: Double-sided tape was used to stick two slides together along their margins. A 50–100 μl volume of Mfp-3S coacervate (0.1 mg $ml^{-1}$) was then injected into the gap and left undisturbed for 1 h to let the coacervate be adsorbed or settle on the glass surfaces. The upper and lower glass slides were then separated and broken into pieces to fit in 1 ml hydrolysis vials. 100 μl of 2 M HCl and 5 μl of phenol were added to the vials containing the glass samples, which were then vacuum sealed, followed by hydrolysis at 158 °C for 1 h. After hydrolysis the solutions were washed twice with water and then twice more with methanol via flash evaporation. The hydrolyzed products were dissolved in 0.02 M HCl and routine amino acid analysis carried out in a Hitachi L-8900 amino acid analyzer.

### 2.6. Adhesion measurement using a Surface Forces Apparatus (SFA)

The adhesion of Mfp-3S coacervate on mica was measured using a SFA. The details of the SFA technique have been described elsewhere [22]. Coacervate deposition was carried out by placing 40 μl of Mfp-3S coacervate (0.1 mg $ml^{-1}$) between two mica surfaces. After 1 h settlement and absorption the bottom mica surface were brought in contact with the upper one, and further compressed for another 1 min before separation All experiments were performed at room temperature, thermostatted at 22 °C.

### 2.7. Quartz crystal microbalance dissipation (QCM-D)

Gold sensors were purchased from BiolinScientific (QSX301) and cleaned according to the protocol suggested before use. QCM-D experiments were carried out in a Q-Sense E4 system using two flow modules in parallel. Samples were introduced into the

modules at a flow rate of 0.1 ml $min^{-1}$ using a four channel Ismatec IPC-N 4 peristaltic pump. In QCM-D changes in resonance frequency ($\Delta F$) and dissipation ($\Delta D$) of a quartz crystal are recorded to measure the amount and viscoelastic properties, respectively, of a material deposited on the sensor. The crystal is excited at its fundamental frequency, approximately 5 MHz, and changes can be observed at the fundamental ($n = 1$) as well as overtone frequencies ($n = 3$, 5, 7, 9, and 11). Readings taken at the fundamental frequency are not usually used as they are prone to artifacts from the sensor clamp.

## 3. Results and discussion

### 3.1. Characterization of the Mfp-3S coacervate morphology

Coacervation is typically measured by turbidimetry, as turbidity increases when macromolecules associate to form phase-separated fluidic droplets. Protein precipitation also leads to turbidity, but the droplet morphology of coacervated macromolecular aggregates is easily distinguished from precipitates by light microscopy (Fig. 2). For the microscopic observation of coacervation and the coalescence of droplets Mfp-3S coacervates were pre-formed in pH 5.5 acetate buffer then injected into the gap between two glass slides.

Fig. 2a, b, d and e) shows bright field microscope images of coacervate droplets that had settled on the bottom slide. As time elapsed more coacervate settled and was adsorbed on the bottom surface, with a lesser amount adsorbed on the upper surface. Using amino acid analysis to quantify coacervate deposition on the two surfaces (upper/lower ratio 0.25–0.20, Fig. 3) following bulk depletion we estimated how readily the coacervate was adsorbed on glass (upper surface) relative to gravity-dependent droplet settlement (lower surface). Visualizing macromolecules in coacervates usually requires functionalization with molecular, often fluorescent, probes, however, this is unnecessary with Mfp-3S as it contains 10 mol.% tryptophan (Trp), which imparts an intense intrinsic fluorescence. With UV excitation (Fig. 2c) Mfp-3S-derived coacervates are readily visualized under microscopic observation.

### 3.2. The effects of buffer pH, ionic strength, and temperature on coacervation

The turbidity of the Mfp-3S dispersions was measured to quantify the yield of coacervate under different buffer conditions. Fig. 4a shows the data collected 1 min after mixing the protein stock and buffer. In the range of pH and ionic strengths tested (avoiding those pH regimes where dopa residues are highly vulnerable to autoxidation) the turbidity was found to increase with pH and ionic strength, and above a certain "critical" pH or ionic strength the protein precipitated from solution. Given the apparent pI for Mfp-3S of ~7.5 from the zeta potential measurements (compared with a predicted pI of ~8 using ExPAsy), the protein is well dispersed in buffer at pH 3 and low monovalent salt concentrations (~10 mM) due to long-range electric double-layer repulsion between the net positively charged molecules. At high ionic strength electrostatic "double-layer" repulsion is largely screened. As the buffering pH is increased and approaches the pI of ~7.5 (the pH at which the positive and negative charges exposed on the molecule surface exactly neutralize each other) the net charge of the Mfp-3S molecules decreases to zero, with a corresponding decrease in and eventual disappearance of long-range double-layer repulsion. Any two contacting droplet surfaces now expose an equal number of positive and negative charges, and coulombic interactions can form between the two surfaces resulting in strong intermolecular attraction. In summary, increasing both the pH and ionic strength leads to decreasing long-range repulsion and increasing short-range attraction (binding adhesion) that results in coalescence of the soluble proteins, first as coacervates and then as precipitates.

Given the observed dependence on pH and ionic strength, electrostatic interactions definitely contribute to Mfp-3S coacervation.

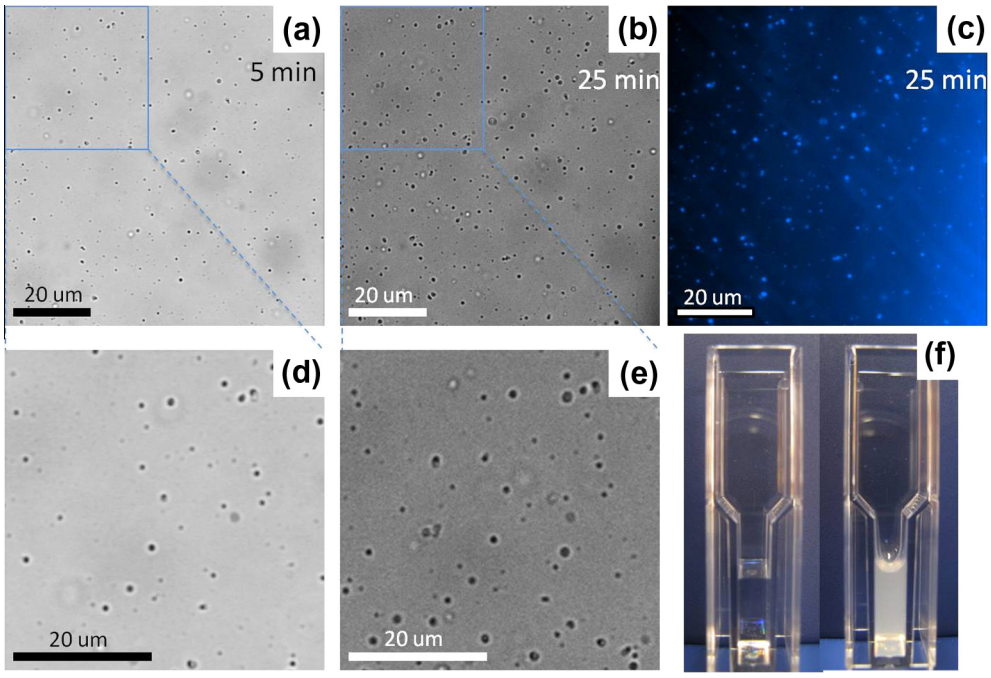


**Fig. 2.** Visualization of coacervation using light microscopy and spectrometry. (a–c) Microscope images of Mfp-3S coacervates taken (a) 5 and (b, c) 25 min after injecting samples into cells for imagin: (a, b) bright field images; (c) fluorescence image. The 5 min time point was selected on the basis of convenience as it was easily obtained after injecting the coacervate between the glass slides. The 25 min time point was chosen as the second time point as there is no discernible change in the adsorbed coacervate droplets after 25 min. (d, e) Enlargements of (a) and (b) respectively. (f) Comparison of Mfp-3S in dispersed solution (left) and associated coacervate (right).

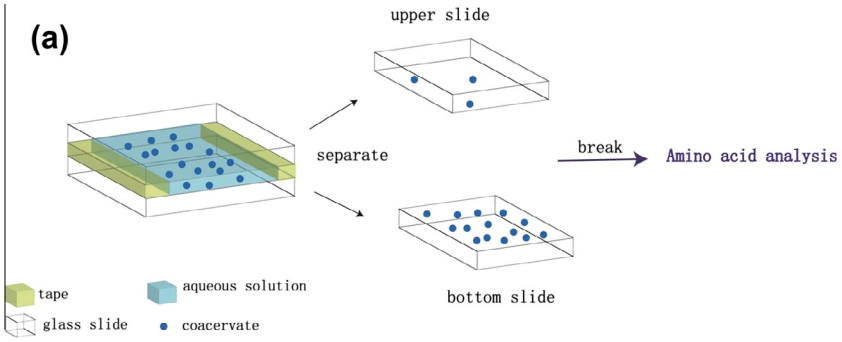


(b)

| | | Asp (nmol) | Gly (nmol) | Tyr (nmol) | Lys (nmol) |
|---|---|---|---|---|---|
| Sample 1 | upper | 0.74 | 1.19 | 0.31 | 0.15 |
| | bottom | 3.98 | 6.05 | 1.69 | 0.78 |
| | u/b ratio | 1/5.4 | 1/5.1 | 1/5.4 | 1/5.2 |
| Sample 2 | upper | 0.94 | 1.65 | 0.43 | 0.17 |
| | bottom | 3.95 | 6.15 | 2.09 | 0.82 |
| | u/b ratio | 1/4.2 | 1/3.7 | 1/4.8 | 1/4.8 |
| Sample 3 | upper | 1.37 | 2.28 | 0.73 | 0.26 |
| | bottom | 5.3 | 8.18 | 2.88 | 1.05 |
| | u/b ratio | 1/3.9 | 1/3.6 | 1/4.0 | 1/4.0 |

**Fig. 3.** (a) Schematic comparison of coacervate yields on the upper and surfaces, which are caused by adsorption only and a combination of adsorption and settlement, respectively. (b) Amino acid analysis results of three pairs of samples.

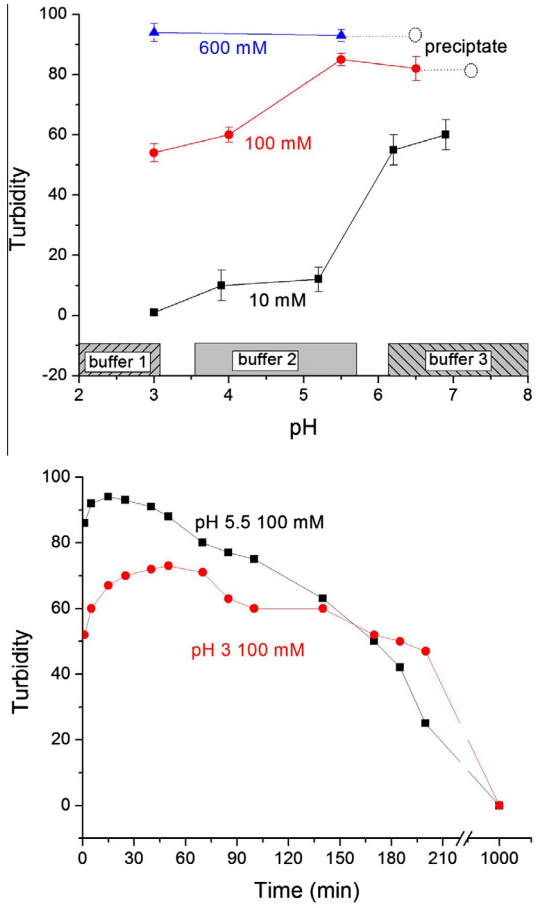


**Fig. 4.** Dependence of coacervate-associated turbidity on pH and time. Turbidity of 0.1 mg ml$^{-1}$ Mfp-3S under different buffer conditions. Buffer 1, phosphate buffer; buffer 2, acetate buffer; buffer 3, phosphate buffer.

Fig. 4b shows the turbidity changes with time. Upon suspension in aqueous solution at a pH and ionic strength suitable for coacervation the Mfp-3S molecules initially phase separate as coacervate droplets. As the droplet size increases so does the turbidity of the solution, peaking at around 30 min. However, after additional time the coacervate droplets settle onto the surface of the enclosure due to their higher density. In addition, the low interfacial energy causes the droplets to spread out upon contact with any surface. The decrease in turbidity after 30 min thus reflects bulk depletion of the coacervate droplets by sedimentation and surface adherence, rather than resolubilization of the Mfp-3S coacervates.

The influence of temperature on Mfp-3S coacervation was also examined. As shown in Table 1, turbidity decreases dramatically with temperature $T$. Previous studies have determined that $T$ affects coacervation according to the driving forces involved: in electrostatically driven complex coacervation increasing $T$ typically decreases the turbidity due to the weaker attraction with increasing $T$ [23], whereas for hydrophobically driven coacervates such as elastin raising $T$ leads to higher turbidity due to entropy-driven association of the molecules [18]. As such, the changes in turbidity reflect the net energy balance of these different trends. For this study the decrease in electrostatic interaction at higher $T$ is such that they appear to overcome the entropy gain at higher $T$ to result in decreased turbidity.

Mfp-3S is the most hydrophobic of all known mussel adhesive proteins, with at least 60% of the amino acid residues in the sequence being more hydrophobic than glycine [17]. The contributions of hydrophobic interactions to the coacervation of Mfp-3S must thus be considered. Fig. 5 compares macromolecular interactions in three different coacervating systems: (1) typical polyca-

**Table 1**
Mfp-3S (0.1 mg ml$^{-1}$) coacervate turbidity change with temperature.

| Turbidity change with T | Room T 18 °C | 37 °C | 50 °C | 70 °C | 80 °C |
|---|---|---|---|---|---|
| pH 5.3 10 mM | 14 | 3 | – | – | – |
| pH 6.2 100 mM | 86 | 80 | 61 | 36 | 27 |

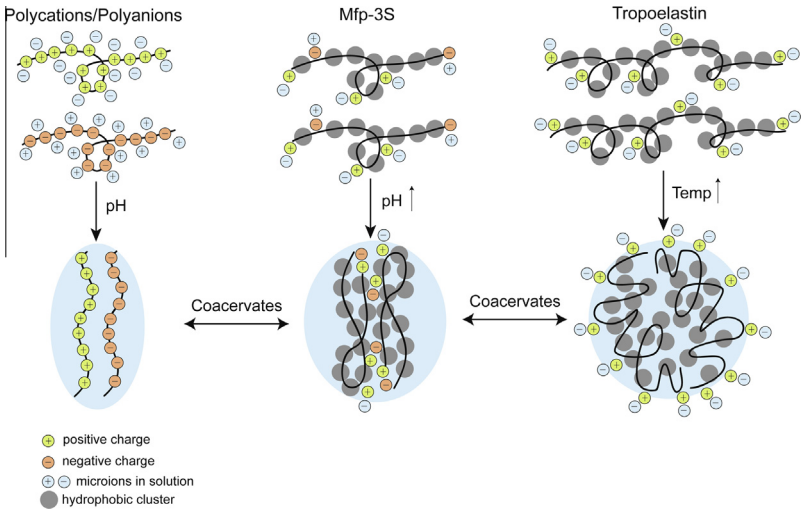


**Fig. 5.** A scheme comparing three different coacervation systems: one complex coacervate and two single component coacervates. (Left) The coacervation of oppositely charged polyelectrolytes occurs under pH conditions at which the net charge of the complex is neutral. (Middle) In Mfp-3S increasing pH deprotonates the carboxylic groups of Asp and the C-terminus ($pK_a \sim 4$) resulting in a zwitterion. Driven by intermolecular charge coupling and hydrophobic interactions between hydrophobic domains, the zwitterionic proteins associate to form coacervates. Hydrophobic interaction is responsible for overcoming the intermolecular electrostatic repulsion caused by the extra positive charge when the pH is lower than the pI of Mfp-3s. In contrast, the self-coacervation of tropoelastin (pI > 10) at any given pH is induced by increasing temperature. Note that Lys charges (⊕) are excluded from the coacervate and neutralized by ions at the surface [35]. Molecules are not drawn to scale. The blue background represents the coacervate defined by the macromolecule complex, the shape of which is arbitrary.

tion/polyanion complex coacervation; (2) Mfp-3S; (3) tropoelastin single component coacervation. The optimum pH for complex coacervation by oppositely charged polyelectrolytes is that at which the polyanions and polycations (such as gelatin and gum Arabic) neutralize one another and intermolecular electrostatic attraction is strongest. In contrast, as pH increases long-range repulsion between Mfp-3S is only partially overcome (complete internal neutralization occurs only when the N-terminus loses a $H^+$ at pH $\geqslant$ 7.5). Even before reaching pH 7.5 the Mfp-3S proteins tend to cluster more freely and may even rearrange to facilitate short-range coupling of positive and negative charges to achieve localized charge neutralization. Given that Mfp-3S coacervation is observed at pH < pI (Fig. 4a), protein coalescence cannot depend exclusively on electrostatic interactions between zwitterions, but must also include hydrophobic interactions between the numerous hydrophobic domains. However, hydrophobic interactions do not contribute to Mfp-3S coacervation in the same way as they do in the coacervation of elastin, which exhibits increased coacervation with increasing $T$ [24], the opposite trend to Mfp-3S, as discussed earlier. In tropoelastin increasing $T$ is essential for the entropy-driven aggregation of hydrophobic domains that simultaneously excludes positive charges from the hydrophobic core (Fig. 5). There are no other reports of single proteins that phase separate by coacervation, indeed, proteins typically precipitate when pH = pI. However, coacervation by zwitterionic gemini surfactants has been observed [26]. These surfactants are, in a way, miniature versions of Mfp-3S in having both positive and negative charges separated by a neutral core domain and terminal non-polar hydrocarbon tails [25]. These features were shown to be critical for coacervation and hence corroborate our model for Mfp-3S coacervation.

### 3.3. Interfacial energy and wettability of the Mfp-3S coacervate

Coacervates with coating or adhesive functions should exhibit a low interfacial energy or tension. The adhesive capillary force of the Mfp-3S coacervate was measured using the SFA as follows. Coacervate preformed in buffer at pH 5.5 was injected between two well-separated mica surfaces and given 1 h to equilibrate, adsorb, and coalesce (spread) on the mica surfaces before performing any measurements. Then the lower mica surface was brought into contact with the upper surface and further compressed for 1 min to allow the coacervate layers on the two surfaces to coalesce, forming a capillary bridge or neck. The bumpy fringe shown in Fig. 6a is an indication of a rough surface and heterogeneous structure/morphology of the coacervate layers and bridging neck. Upon separation, normalized "separation forces" (also "pull-off" or "adhesion" forces) ranging from $F/R = -8$ to $-20$ mN m$^{-1}$ were measured depending on the pulling rate (5–35 nm s$^{-1}$). The effective interfacial energy $\gamma_{eff}$ can then be deduced from the measured adhesion forces $F$ and the radius of curvature $R$ using:

$$\gamma_{eff} = F/3\pi R \quad (1)$$

The interfacial energy $\gamma_{eff}$ was calculated to be in the range 0.5–3.7 mJ m$^{-2}$. Such a low interfacial energy is consistent with that of other coacervates [7,27] and is of significance in adhesion, since the ability to spontaneously wet and spread over a surface is the hallmark of a good adhesive and is reliant on a low interfacial tension. Another demonstration of good wettability is the "anti-coffee ring" effect [28] shown by the Mfp-3S coacervate (Fig. 7), where instead of forming a ring-like deposit along the perimeter of air-dried droplets (as Mfp-3S does in solution) the Mfp-3S coacervate uniformly stains the glass substrate. Given that many applications in printing [29], biology [30], and complex assembly [31] require uniform coatings, Mfp-3S coacervates represent a new class of "complex fluid" coating materials.

### 3.4. Adsorption of the Mfp-3S coacervate on HAP determined by QCM-D

HAP is a bioceramic analog of the mineral component of human bone and teeth. Understanding the interaction between coacervates made of dopa-rich mfps and the surface of HAP could inspire the design of improved medical adhesives and implant surfaces. QCM-D was used here to investigate the adsorption of Mfp-3S coacervates on HAP surfaces, which was compared with the adsorption performance of Mfp-3S in solution and lysozyme (Fig. 8). Mfp-3S in solution or in coacervated form was obtained by using different buffer conditions. Given that the frequency

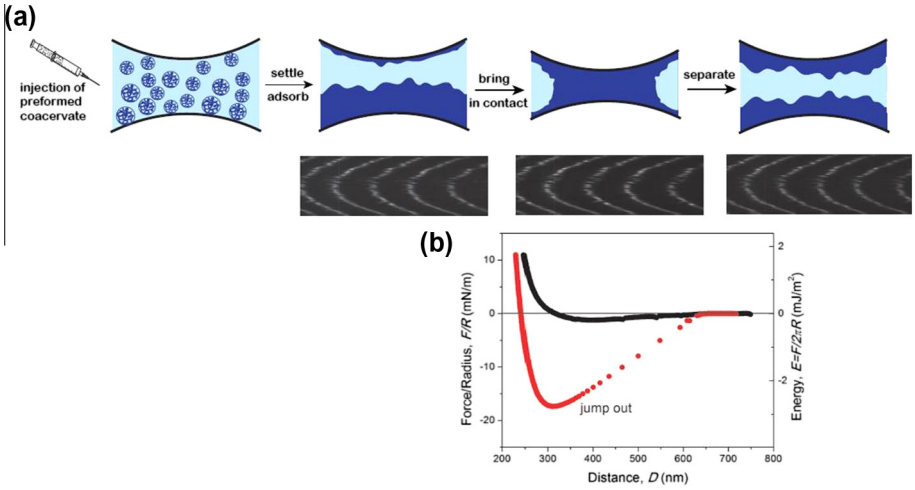


**Fig. 6.** (a) Schematic of the SFA adhesion experiment and corresponding FECO (Fringes of Equal Chromatic Order) patterns in each step; (b) a representative force run plot at 35 nm $s^{-1}$ pulling rate.

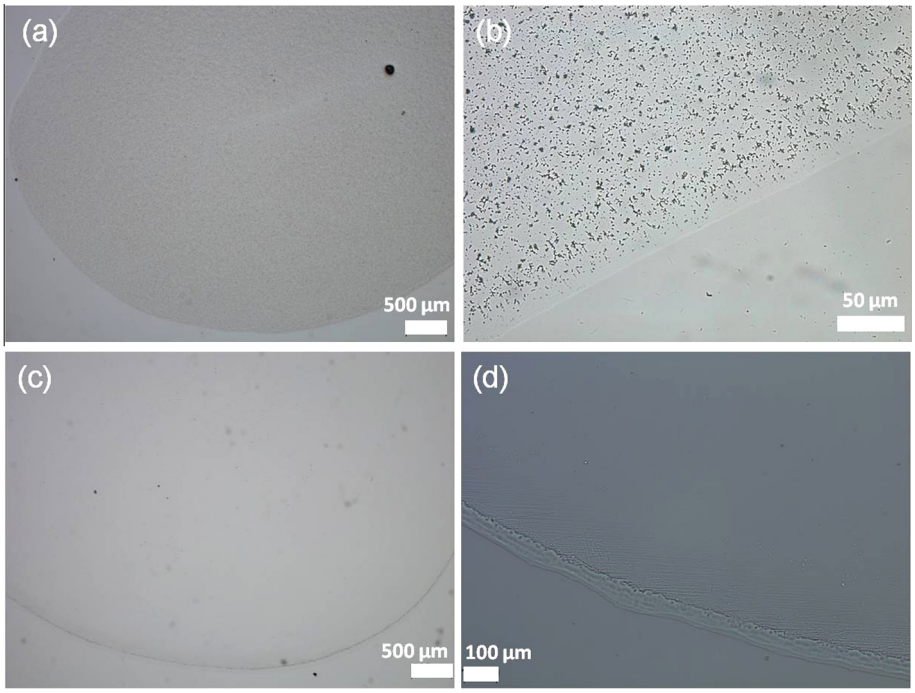


**Fig. 7.** Microscope images of a "coffee stain" left by 10 μl of (a, b) Mfp-3S coacervate and (c, d) Mfp-3S solution, which show "anti-coffee ring" and "coffee ring" effects, respectively. The "anti-coffee ring" effect of the Mfp-3S coacervate indicates a uniform wetting capability.

change $\Delta F$ is proportional to the mass change it is clear that the amount of adsorbed lysozyme is lowest among all the tested samples. Mfp-3S solution shows higher adsorption on HAP than lysozyme, but much less than coacervated Mfp-3S.

Two coacervate samples prepared under different conditions were tested: pH 5.5/ionic strength 100 mM (the "optimized" coacervate, i.e. optimum conditions for Mfp-3S coacervation as indicated by turbidity measurements); pH 3/ionic strength 100 mM ("non-optimized" coacervate, sub-optimal conditions). As expected (Fig. 8a), the optimized coacervates exhibited better adsorption than the non-optimized ones. After rinsing with buffer the mass loss of the optimized coacervate was only 20%, compared with 75% loss of the suboptimal coacervate. Based on these results coacervated Mfp-3S demonstrated excellent adsorption on HAP, primarily based on electrostatic and hydrogen bonding interactions between the protein and HAP, and also interactions between the proteins themselves, which drive the continuous build-up of protein on top of the first protein layer adsorbed to the HAP surface. The interaction between protein and HAP is likely to be mainly hydrogen bonding between the protein dopa and the phosphate groups on HAP, enhanced by electrostatic interaction between the positively charged protein and net negatively charged HAP surface. It is expected that dopa–phosphate hydrogen bonding will be weaker at pH 5.5 than at pH 3 due to dopa autoxidation [32,33]. The adsorption of lysozyme (pI ~ 11) on HAP appeared independent of the buffer pH used, which is consistent with electrostatic interactions between phosphate groups and lysine and arginine, whose charges would not change in the pH range tested given the reported $pK_a$ values of 10.4 and 12.5, respectively [34]. Considering that both lysozyme and Mfp-3S are basic, electrostatic interactions between Mfp-3S and HAP under all three buffer conditions is unlikely to be the major reason for the differences in

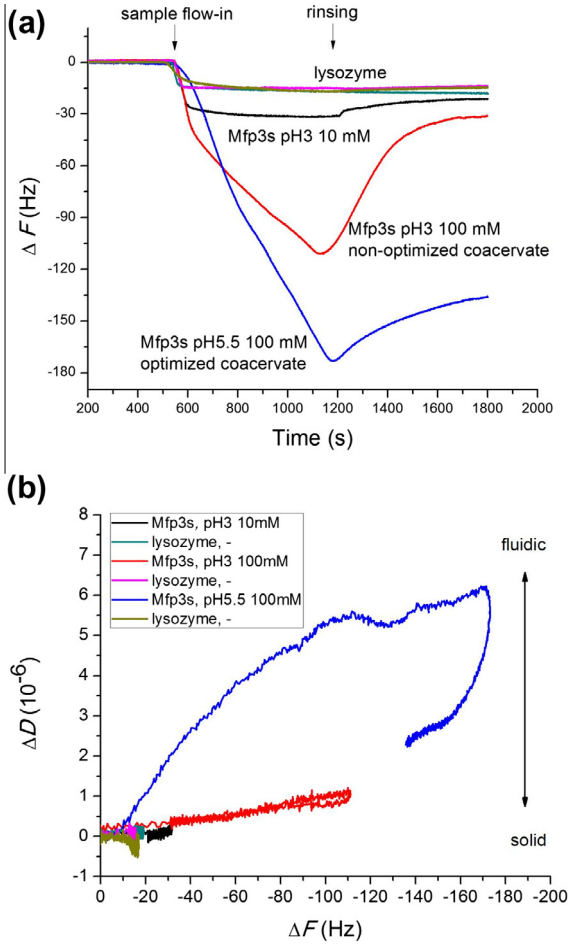


**Fig. 8.** (a) Changes in frequency in QCM-D experiments after exposing a HAP surface to Mfp-3S solution (pH 3, 10 mM), coacervate (pH 3 100 mM and pH 5.5 100 mM) and lysozyme solution under the above three conditions. (b) Plots of $\Delta D$ vs. $\Delta F$. The higher $\Delta D/\Delta F$ the softer the material.

adsorption. From these results it can be inferred that the highest adsorption of "optimized" Mfp-3S coacervate and lowest mass loss during rinsing (compared with non-optimized coacervate) are due to the same strong intermolecular interactions (cohesion) that also drive protein coacervation. The dissipative change $\Delta D$ is an indication of a material's viscoelastic properties. The higher $\Delta D$ the more fluidic, or "softer", the material is; the lower $\Delta D$ the more solid, or "stiffer", the material is. It is clear from Fig. 6b that the absorbed layer of coacervate is the most fluidic of all the tested samples, to the extent that changes in $\Delta D$ represent changes in viscosity. The significant hysteresis exhibited by the coacervate suggests that it may be ideally suited for dissipating energy associated with deformation of the adhesive plaque produced by drag and lift forces.

## 4. Conclusion

Mfp-3S is the first known naturally occurring self-coacervating adhesive protein from the mussel and, along with tropoelastin, the only protein known to self-coacervate. In marked contrast to elastin coacervation, which is hydrophobically driven, the phase separation of Mfp-3S is markedly dependent on ionic strength and pH, the hallmarks of complex coacervation, but unlike the coacervation of gelatin and gum Arabic, for example, is optimal at pH values below those necessary for protein charge neutralization. Conditions for Mfp-3S coacervation are perfectly adapted for the solution conditions that exist under the foot during plaque formation, namely an acidic pH at ~0.1 M ionic strength [33]. Electrostatic and hydrophobic interactions between and within Mfp-3S under these conditions drive the association of protein molecules to form a fluid phase that is separate from bulk water. One component coacervates formed by Mfp-3S may circumvent much of the instability and complicated solution chemistry associated with binary and ternary coacervates. Given the low interfacial energy of coacervated Mfp-3S and its superior adsorption on HAP surfaces shown by the SFA and QCM-D experiments, respectively, it is highly likely that the coacervates formed from recombinant Mfp-3S or its synthetic analogs can be used in future investigations to explore potential dental or orthopaedic adhesive applications.

## Acknowledgements

This research was supported by the MRSEC Program of the National Science Foundation under award no. DMR 1121053 and by NIH grant R01 DE018468. We thank Dr Matthew Dixon (Biolin Scientific) and Dr Mary Raven (NRI/MCDB Microscopy Facility, UCSB) for their help with the QCM-D measurements and microscope training, respectively.

## Appendix A. Figures with essential colour discrimination

Certain figures in this article, particularly Figs. 1–8, are difficult to interpret in black and white. The full colour images can be found in the on-line version, at http://dx.doi.org/10.1016/j.actbio.2013.09.007.

## References

[1] Bungenberg de Jong HG. Die Koazervation und ihre Bedeutung für die Biologie. Protoplasma 1932;15:110–73.
[2] Bungenberg de Jong HG. Complex colloid systems. In: Colloid science. Amsterdam: Elsevier; 1949.
[3] Cooper CL, Dubin PL, Kayitmazer AB, Turksen S. Polyelectrolyte–protein complexes. Curr Opin Colloid Interface Sci 2005;10:52–78.
[4] Waite JH, Andersen NH, Jewhurst S, Sun CJ. Mussel adhesion: finding the tricks worth mimicking. J Adhesion 2005;81:297–317.
[5] Kausik R, Srivastava A, Korevaar PA, Stucky G, Waite JH, Han S. Local water dynamics in coacervated polyelectrolytes monitored through dynamic nuclear polarization-enhanced (1)H NMR. Macromolecules 2009;42:7404–12.
[6] Srivastava A, Waite JH, Stucky GD, Mikhailovsky A. Fluorescence investigations into complex coacervation between polyvinylimidazole and sodium alginate. Macromolecules 2009;42:2168–76.
[7] Hwang DS, Zeng HB, Srivastava A, Krogstad DV, Tirrell M, Israelachvili JN, et al. Viscosity and interfacial properties in a mussel-inspired adhesive coacervate. Soft Matter 2010;6:3232–6.
[8] Shao H, Stewart RJ. Biomimetic underwater adhesives with environmentally triggered setting mechanisms. Adv Mater 2010;22:729–33.
[9] Torrent J, Alvarez-Martinez MT, Harricane MC, Heitz F, Liautard JP, Balny C, et al. High pressure induces scrapie-like prion protein misfolding and amyloid fibril formation. Biochemistry 2004;43:7162–70.
[10] Weinbreck F, Minor M, De Kruif CG. Microencapsulation of oils using whey protein/gum arabic coacervates. J Microencapsul 2004;21:667–79.
[11] Tuinier R, ten Grotenhuis E, de Kruif CG. The effect of depolymerised guar gum on the stability of skim milk. Food Hydrocolloid 2000;14:1–7.
[12] de Kruif CG, Tuinier R. Polysaccharide protein interactions. Food Hydrocolloid 2001;15:555–63.
[13] Ganzevles RA, Kosters H, van Vliet T, Stuart MAC, de Jongh HHJ. Polysaccharide charge density regulating protein adsorption to air/water interfaces by protein/polysaccharide complex formation. J Phys Chem B 2007;111:12969–76.
[14] Dickinson E. Interfacial structure and stability of food emulsions as affected by protein–polysaccharide interactions. Soft Matter 2008;4:932–42.
[15] Tokarev I, Minko S. Stimuli-responsive porous hydrogels at interfaces for molecular filtration, separation, controlled release, and gating in capsules and membranes. Adv Mater 2010;22:3446–62.
[16] Hunt JN, Feldman KE, Lynd NA, Deek J, Campos LM, Spruell JM, et al. Tunable, high modulus hydrogels driven by ionic coacervation. Adv Mater 2011;23:2327–31.
[17] Wei W, Yu J, Broomell C, Israelachvili JN, Waite JH. Hydrophobic enhancement of dopa-mediated adhesion in a mussel foot protein. J Am Chem Soc 2013;135:377–83.

[18] Urry DW, Trapane TL, Prasad KU. Phase-structure transitions of the elastin polypentapeptide water-system within the framework of composition temperature studies. Biopolymers 1985;24:2345–56.
[19] Kaibara K, Sakai K, Okamoto K, Uemura Y, Miyakawa K, Kondo M. Alpha-elastin coacervate as a protein liquid membrane – effect of pH on transmembrane potential responses. Biopolymers 1992;32:1173–80.
[20] Zhao H, Robertson NB, Jewhurst SA, Waite JH. Probing the adhesive footprints of *Mytilus californianus* byssus. J Biol Chem 2006;281:11090–6.
[21] Hwang DS, Waite JH, Tirrell M. Promotion of osteoblast proliferation on complex coacervation-based hyaluronic acid–recombinant mussel adhesive protein coatings on titanium. Biomaterials 2010;31:1080–4.
[22] Israelachvili JN, Adams GE. Measurement of forces between 2 mica surfaces in aqueous-electrolyte solutions in range 0–100 Nm. J Chem Soc Faraday Trans 1978;74:975–1001.
[23] Chollakup R, Smitthipong W, Eisenbach CD, Tirrell M. Phase behavior and coacervation of aqueous poly(acrylic acid)–poly(allylamine) solutions. Macromolecules 2010;43:2518–28.
[24] Vrhovski B, Jensen S, Weiss AS. Coacervation characteristics of recombinant human tropoelastin. Eur J Biochem 1997;250:92–8.
[25] Peresypkin AV, Menger FM. Zwitterionic geminis. Coacervate formation from a single organic compound. Org Lett 1999;1:1347–50.
[26] Priftis D, Farina R, Tirrell M. Interfacial energy of polypeptide complex coacervates measured via capillary adhesion. Langmuir 2012;28:8721–9.
[27] Spruijt E, Sprakel J, Stuart MAC, van der Gucht J. Interfacial tension between a complex coacervate phase and its coexisting aqueous phase. Soft Matter 2010;6:172–8.
[28] Yunker PJ, Still T, Lohr MA, Yodh AG. Suppression of the coffee-ring effect by shape-dependent capillary interactions. Nature 2011;476:308–11.
[29] Park J, Moon J. Control of colloidal particle deposit patterns within picoliter droplets ejected by ink-jet printing. Langmuir 2006;22:3506–13.
[30] Dugas V, Broutin J, Souteyrand E. Droplet evaporation study applied to DNA chip manufacturing. Langmuir 2005;21:9130–6.
[31] Hu H, Larson RG. Marangoni effect reverses coffee-ring depositions. J Phys Chem B 2006;110:7090–4.
[32] Yu J, Wei W, Danner E, Israelachvili JN, Waite JH. Effects of interfacial redox in mussel adhesive protein films on mica. Adv Mater 2011;23:2362.
[33] Yu J, Wei W, Danner E, Ashley RK, Israelachvili JN, Waite JH. Mussel protein adhesion depends on interprotein thiol-mediated redox modulation. Nat Chem Biol 2011;7:588–90.
[34] Figueiredo KCD, Salim VMM, Alves TLM, Pinto JC. Lysozyme adsorption onto different supports: a comparative study. Adsorption 2005;11:131–8.
[35] Yeo GC, Keeley FW, Weiss AS. Coacervation of tropoelastin. Adv Colloid Interface 2011;167:94–103.